



Tree profile equations are significantly improved when adding tree age and stocking degree: an example for *Larix gmelinii* in the Greater Khingan Mountains of Inner Mongolia, northeast China

Yang Liu^{1,2} · Chaofang Yue³ · Xiaohua Wei² · Juan A. Blanco⁴ · Ralph Trancoso⁵

Received: 7 October 2019 / Revised: 17 January 2020 / Accepted: 23 January 2020 / Published online: 3 February 2020
© Springer-Verlag GmbH Germany, part of Springer Nature 2020

Abstract

Tree age (AGE) and stocking degree (P) strongly influence tree shape, but their effects have been neglected in most tree profile equations. In addition, data used to build traditional tree profile equations usually do not meet the statistical requirements of independence and identical distribution of observations. Therefore, our main objectives were to present a method to improve taper equations with measurements easily collected in tree inventories (age, stocking degree) and also improve the statistical accuracy of those equations by selecting parameters with a more rigorous way than what is traditionally being done. We evaluated the effects of incorporating age and stocking degree as regressors in tree profile equations selected among 30 candidate foundation equations and parameterized with data from 1858 *Larix gmelinii* (Rupr.) trees growing in the northern China. We used nonlinear mixed-effects models to minimize statistical problems present when building traditional tree profile equations: lack of independence and identical distribution of observations, random effects related to individual trees. Equations incorporating age and stocking degree significantly improved their accuracy. When the equation parameters were estimated with mixed-effects models containing exponential variance functions and accounting for non-independence of observations from the same tree, diameters at any height along the tree bole were more accurately estimated. We demonstrate a new methodology to build more accurate tree profile equations that could support better economic valorization of timber and improve calculations of carbon flows in forests, not only for natural *L. gmelinii* forest but for other species growing in dense natural stands around the globe.

Keywords Nonlinear mixed-effects model · Single, segmented and variable-form taper functions · Autocorrelation · Heteroscedasticity

Communicated by Thomas Knoke.

Electronic supplementary material The online version of this article (<https://doi.org/10.1007/s10342-020-01261-z>) contains supplementary material, which is available to authorized users.

✉ Juan A. Blanco
juan.blanco@unavarra.es

Yang Liu
liuyangvip@hotmail.com

Chaofang Yue
ChaoFang.Yue@forst.bwl.de

Xiaohua Wei
adam.wei@ubc.ca

Ralph Trancoso
ralphtrancoso@gmail.com

Introduction

Taper equations allow forest managers to estimate timber volume, how the diameter of the stem (over or under bark) changes along the length of the stem (Clutter et al. 1983; West 2009), and the size of various end products (pulpwood,

¹ College of Forestry, Inner Mongolia Agricultural University, Hohhot 010019, China

² Department of Earth, Environmental and Geographic Sciences, University of British Columbia (Okanagan), 1177 Research Road, Kelowna, BC V1V 1V7, Canada

³ Forest Res Inst Baden Wurttemberg, Wonnhaldestr 4, 79100 Freiburg, Germany

⁴ Departamento de Ciencias, Universidad Pública de Navarra, Campus de Arrosadía, 31006 Pamplona, Navarra, Spain

⁵ Global Change Institute, University of Queensland, Brisbane, QLD 4072, Australia

sawlogs, poles, veneer, etc.). Taper equations can be classified into three main categories: (1) single taper equations such as those developed by Kozak et al. (1969), Ormerod (1973), and Sharma and Oderwald (2001); (2) segmented taper equations, as presented by Max and Burkhart (1976) and Farrar (1987); and (3) variable-form taper equations as described by Kozak (1988), Kozak (2004), and Sharma and Parton (2009).

Single taper models describe the taper in a stem based on a single function (Sharma and Oderwald 2001). To save computing time, Kozak (1988) developed the variable-form taper equation, becoming the most researched model type (Bi 2000; Bi and Long 2001; Kozak 2004; Li and Weiskittel 2010). In general, variable-form taper models have shown the lowest bias and the greatest precision in taper predictions of the three types of taper models, followed by segmented and single taper models (Rojo et al. 2005; Sakici et al. 2008).

Taper equations also have to be in accordance with the known tree ecophysiology. The shape of the bole generally shows considerable differences such as straight from top to bottom, satiation, curve (bend), or a sharp and distinct or indistinct trunk. Tree shape is generally influenced by a broad range of factors such as: tree genetic make-up (Larson 1963; Meng 2006), tree characteristics (e.g., age, crown size, position of branch and species) (Gray 1956; Li and Weiskittel 2010; Muhairwe 1993; Muhairwe et al. 1994), stand characteristics (e.g., density and stand age) (Gray 1956; Larson 1963; Muhairwe 1993; Sharma and Zhang 2004), site characteristics (e.g., water and nutrients) (Calama and Montero 2006; Larson 1963; Metzger 1894), climatic factors (e.g., mean annual precipitation and end of frost-free period) (Nigh and Smith 2012; Schneider 2018), and management and land use actions (e.g., thinning and pruning) (Ferreira et al. 2014; Tasissa and Burkhart 1998; Tasissa et al. 1997). These factors play an important role on taper equations as well (Brooks et al. 2008) and have been incorporated as independent variables on top of conventional variables such as total height, diameter at breast height (DBH) and height above the ground. Numerous studies have documented that the addition of crown dimensions-related metrics can improve taper equations' accuracy (Jiang and Liu 2011; Leites and Robinson 2004; Valenti and Cao 1986). However, such improvements in model accuracy depend on the region, species and other aforementioned factors (Burkhart and Walton 1985; Li and Weiskittel 2010; Muhairwe et al. 1994; Valenti and Cao 1986). It is also well known that tree age (AGE) also strongly influences tree stem form because tree growth includes diameter and height from the continued biomass accumulation with increasing AGE (Brooks et al. 2008). Newnham (1965) stated that taper increased most rapidly with AGE in trees grown with heavy thinning.

In addition, several attempts have been made to incorporate tree density (defined as the number of trees per area unit) into taper models (e.g., Sharma and Zhang 2004; Smithers 1961). However, there are two major disadvantages of incorporating tree density into taper profile models. First, available tree density information is usually deficient. For example, only three tree density values were used by both Sharma and Zhang (2004) and Smithers (1961) to assess the effect of tree density on stem form. Second, tree density typically shows a response to stand density worse than the stocking degree (P).

Although other stand or individual tree variables have been previously incorporated to taper equations, few studies have quantitatively examined the effects of introducing AGE or AGE and P simultaneously on taper model accuracy. In addition, the effects of both AGE and P are typically species specific, as each tree species grows at a different rate and into different stem shapes. Therefore, taper equations are limited by species specificities (Li et al. 2012; Sharma and Zhang 2004). It is particularly important to account for that for species not well represented in academic literature, like those from northern China.

While taper equations have been extensively used, a concern is that multiple measurements from an individual tree used in the construction of taper equations may lead to autocorrelation and heteroscedasticity (Lindstrom and Bates 1990), which violate the assumption of independent distribution of observations (Valentine and Gregoire 2001). An early example of introducing random factors in volume equations was provided by Lappi (1991). Nonlinear mixed-effects (NLME) models can solve these problems as they allow a predictive role in two ways, i.e., a typical response (including only fixed-effects parameters) and a calibrated response (including both fixed- and random-effects parameters) (Calama and Montero 2004). NLME models have the advantage of estimating the covariance matrix associated with hierarchical structure data (Garber and Maguire 2003). Additionally, they can use the prior measurement of the diameter within the sample tree to calculate random-effects parameters and then calibrate the taper profile model to the sample tree level (Gómez-García et al. 2013; Trincado and Burkhart 2006).

The forests in the Great Khingan Mountains (Inner Mongolia, northeast China) are among the most sensitive ecosystems to global climate change in China (Fu et al. 2018). These forests are the largest continuous bright coniferous forest of the cold temperate zone in China (Xu 1998), being *Larix gmelinii* (Rupr.) the dominant tree species (Jiang et al. 2002). *Larix gmelinii* forests account for more than 57% of the total Greater Khingan Mountains area, and the volume of *L. gmelinii* forests occupies about 8% of the total standing volume in Chinese forests (DFPRC 2014). These forests have been the focus of research for several years as *L. gmelinii*

is also a major commercial species in Chinese boreal forest (Xu 1998). As the demand for timber has increased during the past decades, accurate determination of stem taper has great interest (Lejeune et al. 2009). However, in spite of its economic and ecological importance, the factors driving *L. gmelinii* stem growth and shape are yet poorly understood. Hence, we attempt to develop specific stem taper equations for *L. gmelinii*, which would help to improve timber volume estimates and carbon sequestration budgets, and as a result, contribute to the sustainable management of these forests.

Given the above mentioned research gaps, we hypothesize that: (1) in the case of natural forests adding the variables AGE and *P* will significantly improve stem taper equations; and (2) using NLME tree profile equations with random effects at tree level will be a successful strategy to remove the issues of heteroscedasticity and autocorrelation from the data structure used to build up the taper models. When testing these two hypotheses, we aim to reach the following objectives: (1) to construct a specific taper equation for *L. gmelinii*; (2) if our first hypothesis is supported, to incorporate AGE and *P* as independent variables into the taper equation to quantitatively analyze their effect on model predictive precision when estimating diameters along the bole; and (3) if our second hypothesis is supported, to develop a NLME taper equation with random effects at tree level to reduce autocorrelation and heteroscedasticity of hierarchical structure data when data are repeatedly measured for the same tree.

Materials and methods

Study area and stem data

The study area is located in the Greater Khingan Mountains of Inner Mongolia, situated in the sub-frigid region with a distinct cold temperate continental monsoon climate (Supplementary Information: Fig. S1). The geographic range of the study area is 119° 36'–125° 19' E, and 47° 3'–53° 20' N. Between 330 and 1750 m.a.s.l., the annual precipitation ranges from 350 to 500 mm, most of which falls in May to October. The mean annual temperature is about $-3\text{ }^{\circ}\text{C}$, and the mean monthly maximum and minimum temperatures are 17 to 20 °C and -20 to $-30\text{ }^{\circ}\text{C}$ in July and January, respectively. Slopes in the region are moderate, being the average slope 10°. Research area's soil type is predominantly a dark brown forest soil. *L. gmelinii* is the dominant tree species. Other tree species include white birch (*Betula platyphylla* Suk.), aspen (*Populus davidiana* Dole), Scots pine (*Pinus sylvestris* L. var. *mongolica* Litv.) and Korean spruce (*Picea koriensis* Nakai). The main forest types include *L. gmelinii*-*Ledum palustre*, *L. gmelinii*-grass and *L. gmelinii*-*Rhododendron dahurica* (Xu 1998).

Data used in this research came from natural *L. gmelinii* stands located in the 17 Forestry Bureaus throughout the Greater Khingan Mountains (Fig. S1), covering the existing *P* range of these forests. A total of 10,729 measured values were taken from 1858 dominant, intermediate and suppressed trees with AGE ranging from 7 to 201 years from 381 plots with areas from 0.04 to 1.05 ha. Trees were felled and measured to model stem shape variability. To validate each model, 2146 data points (20% of total data) were randomly selected as a validation dataset. The remaining data were used for model fitting.

All trees were measured for DBH outside bark (*D*) (diameter at breast height, 1.3 m above the ground) to the nearest 0.1 cm, total tree height (*H*) to the nearest 0.1 m, and diameter outside bark (*d*) at stump height (between 0.1 and 0.3 m above the ground) and at 0.7 m height. Diameter along the stem was measured at 0.5, 1 or 2 m intervals (depending on the total height of the sample trees) from DBH to the tree tip. In each section, two perpendicular diameters outside bark (*d*) were measured and were then arithmetically averaged. Tree age was estimated by counting growth rings at the basal stem section.

The following three indicators were calculated for each tree: $q = h/H$ (relative height), $X = (H - h)/(H - 1.3)$ and $Z = (H - h)/H$. For stand density, *P* is the most accurate indicator in multi-aged stands (O'Hara 2014). In order to calculate *P*, the basal area of the stand was first calculated. Two methods were used to determine the basal area of the stand;

- I. For the first 355 plots, stand basal areas were calculated by positioning a subplot of known area. The diameters at breast height outside bark of all the trees in the subplot were measured. The diameters were then converted to stem cross-sectional areas; the results were summed and divided by the plot area to give stand basal area.
- II. For the last 26 plots that were set up, stand basal areas were measured using the self-leveling stick type angle gauge (angle count sampling), using a basal area factor (F_g) of 1 m²/ha. The principles of this method can be found in Bitterlich (1984).

The *P* value of each stand was determined using the basal area of the current stand divided by the basal area of the standard yield stand ($P = 1$), which was estimated based on a standard table of the basal area–volume for natural *L. gmelinii* under the same site conditions (Agriculture and Forestry Planning Team of Inner Mongolia Autonomous Region 1974). Summary statistics for *D*, *H*, AGE and *P* of sample trees used in fitting and validating the models are described in Table 1. Figure 1 shows the variation magnitude between the relative height and relative diameter (d/D) according to measurement data points of the 1858 trees.

Table 1 Summary statistics for *Larix gmelinii* tree attributes for the model fitting (1486 trees) and validation (372 trees) data

Variable	Fitting				Validation				
	Mean	SD	Min	Max	Mean	SD	Min	Max	
No. of data points = 8583					No. of data points = 2146				
<i>D</i> (cm)	16.3	6.9	1.0	68.3	16.4	7.2	2.1	68.3	
<i>H</i> (m)	15.3	4.1	2.0	43.0	15.3	4.3	3.2	41.9	
AGE (a)	25	32	7	200	27	35	10	201	
<i>P</i>	0.63	0.14	0.27	0.96	0.64	0.12	0.32	0.94	

D diameter at breast height outside bark; *H* total tree height; AGE tree age; *P* stocking degree. *Min* minimum; *Max* maximum; *SD* standard deviation

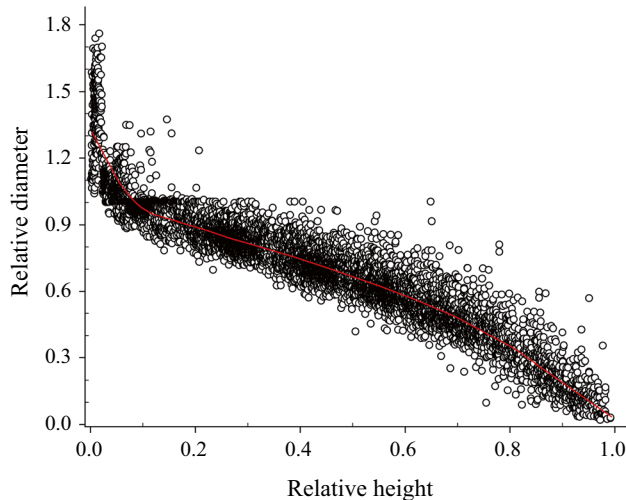


Fig. 1 Scatter plot of the relative height over relative diameter of 10,729 data points for 1858 *Larix gmelinii* (Rupr.) trees

Stem taper foundation equation

Thirty different taper equations were used (Table S1). The first sixteen taper equations are single taper models, the middle four equations are segmented taper models, and the last ten taper equations are variable-form taper models. All the foundation stem taper models were fitted with the nonlinear least squares using the *nlme* package in R (Pinheiro et al. 2018). The Newberry and Burkhart (1986), Max and Burkhart (1976) and Kozak (2004)-(2) models were superior to the other models in predicting diameter outside bark of *Larix gmelinii* for the single, segmented and variable-form taper models, respectively. However, the Max and Burkhart (1976) model displayed the smallest R^2_{adj} and the largest RMSE, MAB and MPRB for both fitting and validation, when compared with the other two models mentioned above. Therefore, the Newberry and Burkhart (1986) and Kozak (2004)-(2) models were selected in this study as the foundation models for further incorporation of AGE and *P*, and for developing NLME single and variable-form taper models,

respectively. The best single taper foundation model selected was [Eq. (1)]:

$$d_{ij} = b_1 D_i \left(\frac{H_i - h_{ij}}{H_i - 1.3} \right)^{b_2} + \varepsilon_{ij} \quad (1)$$

The best variable-form taper foundation model selected was [Eq. (2)]:

$$d_{ij} = b_1 D_i^{b_2} H_i^{b_3} x_{ij} \left[b_4 q_{ij}^{b_5} + b_5 [1/e^{D_i/H_i}] + b_6 x_{ij}^{0.1} + b_7 (1/D_i) + b_8 H_i^{(1-q_{ij}^{1/3})} + b_9 x_{ij} \right] + \varepsilon_{ij} \quad (2)$$

where d_{ij} (cm) is diameter outside bark at a height h_{ij} of the *j*th measurement in the *i*th tree; D_i (cm) and H_i (m) are the DBH outside bark and total tree height of the *i*th tree, respectively; $x_{ij} = (1 - q_{ij}^{1/3}) / (1 - (1.3/H_i)^{1/3})$, $q_{ij} = h_{ij}/H_i$; ε_{ij} is an error term; and b_1 – b_9 are model parameters.

Additional AGE and *P* variables as regressors in stem taper foundation equations

A univariate ANOVA was used to test whether relative diameters were statistically different for AGE and *P*. The relative height (independent variable) was divided into ten sections. Within each section, AGE was divided into five different classes, following the standard set by the State Forestry Administration of the P.R. China (SFAPRC 2011, see Appendix 1 in Supplementary Information for a detailed explanation of how age classes are defined). The AGE classes were as follows: young (0–40 years), half-mature (41–80 years), near mature (81–100 years), mature (101–140 years) and over mature (> 141 years). The *P* values of the stands were equally divided into three different density classes as follows: low (0.10–0.39), middle (0.40–0.69) and high (> 0.7). Before data analysis, boxplots and histograms were used to detect possible outliers and to determine the skewness of the data (Liu et al. 2014). Differences among groups of AGE and *P* were tested with Tukey's honest significant difference test. A *p* value of 0.05 or less was defined as statistically significant.

Pearson’s correlation coefficient was calculated to measure the relationship between the dependent variable (d) and AGE and P (independent variables). Scatter plots were used to seek the relationship between the relative diameter and AGE and P . To avoid bias on model selection by the use of pre-selected regressor type on AGE or P in the taper equation, several forms of linear, power, exponential, and logarithmic models and their combinations for AGE and P were repeatedly tested by adding them into the best-fitted foundation model identified for *L. gmelinii* to validate the performance and identify the most suitable form of the variables AGE and P in the best-fitted foundation models. Comparisons were made among fitted models with different forms for AGE and P in terms of the Akaike’s information criterion (AIC), Bayesian information criterion (BIC) and log likelihood (logLik) (Sakamoto et al. 1986; Schwarz 1978; Yang et al. 2009b) for the stem diameter predictions.

Nonlinear mixed-effects (NLME) models

NLME models contain both fixed-effects parameters common to all individuals and random-effects parameters specific for each individual. Hence, the most important step in the construction of the NLME models is to determine which parameters are the fixed-effects parameters and which parameters are the mixed-effects (both fixed and random effects) parameters. The most common method to determine the parameter status is to fit the same tree profile model with possible combinations of fixed- and random-effects parameters and to select as the optimal fitted mixed-effects model the one with the smallest AIC and BIC. The mixed-effects model fitting was performed with restricted maximum likelihood using the *nlme* function of the *nlme* package in R v. 3.5.2 (R Development Core Team 2017).

Datasets of tree profile equations were compiled from different points along the same individual tree stem, thus leading to the two problems of heteroscedasticity and autocorrelation usually identified in common taper equations (Neter et al. 1996). Heteroscedasticity and autocorrelation can be handled by incorporating individual tree as a random effect into NLME models of tree profile to accurately predict stem diameters at any h value (Garber and Maguire 2003; Pinheiro and Bates 2000). The expression of NLME models was as follows Eq. (3):

$$\mathbf{d}_i = f(\boldsymbol{\theta}_i, \mathbf{X}_i) + \boldsymbol{\varepsilon}_i \tag{3}$$

where \mathbf{d}_i is the vector for diameter outside bark at the different heights h on the i th tree (dependent variable); \mathbf{X}_i is the vector for the independent variable; $\boldsymbol{\theta}_i$ is the parameter vector of fixed and random effects for the NLME model, $\boldsymbol{\theta}_i = \mathbf{A}_i\boldsymbol{\beta} + \mathbf{B}_i\mathbf{u}_i$; $\boldsymbol{\beta}$ is the vector of fixed parameters with design matrix \mathbf{A}_i ; \mathbf{B}_i is the random-effects design matrix for

the sample tree; \mathbf{u}_i is the vector of random effects for sample tree, $\mathbf{u}_i \sim N(0, \mathbf{D})$, where N is the multivariate normal distribution and \mathbf{D} is the variance–covariance structure matrix for the random-effects parameters \mathbf{u}_i , which explains between-tree random variability, and is considered common to every tree analyzed (Calama and Montero 2005).

Under these conditions, the \mathbf{D} matrix, which must be a positive semidefinite matrix, is generally considered as the unstructured positive definite matrix in forest research (Dong et al. 2016; Pinheiro and Bates 2000; Yang et al. 2009b). We also used our dataset of stem taper to show that the evaluation indices, AIC and BIC, are the smallest when the \mathbf{D} matrix is the unstructured positive matrix. \mathbf{D} can be expressed as follows Eq. (4):

$$\mathbf{D} = \begin{pmatrix} \sigma_1^2 & \text{Corr}_{12}\sigma_1\sigma_2 & \cdots & \text{Corr}_{1n}\sigma_1\sigma_n \\ \text{Corr}_{12}\sigma_1\sigma_2 & \sigma_2^2 & \cdots & \text{Corr}_{2n}\sigma_2\sigma_n \\ \vdots & \vdots & \ddots & \vdots \\ \text{Corr}_{1n}\sigma_1\sigma_n & \text{Corr}_{2n}\sigma_2\sigma_n & \cdots & \sigma_n^2 \end{pmatrix} \tag{4}$$

where σ_1 , σ_2 and σ_n represent the standard deviation of the first, second and n th random effects, respectively; Corr_{12} , Corr_{1n} and Corr_{2n} are the correlation coefficient between the first and second random effects, the first and n th random effects and the second and n th random effects; $\boldsymbol{\varepsilon}_i$ is random error, $\boldsymbol{\varepsilon}_i \sim N(0, \mathbf{R}_i)$, where \mathbf{R}_i is the within-tree variance–covariance matrix, which needs to be specified to account for any within-tree heteroscedasticity and autocorrelation among measurements. \mathbf{R}_i can be expressed as follows:

$$\mathbf{R}_i = \sigma^2 \mathbf{G}_i^{0.5} \boldsymbol{\Gamma}_i \mathbf{G}_i^{0.5} \tag{5}$$

where σ^2 is a scaling factor for error dispersion which was given by the value of residual variance of the estimated model; \mathbf{G}_i is the diagonal matrix explaining the variance of within-tree heteroscedasticity; and $\boldsymbol{\Gamma}_i$ is a matrix accounting for within-tree autocorrelation structure of the errors.

To correct the within-tree heteroscedasticity, we utilized a power of the fitted value (\hat{d}) variance function, $\text{Var}(\boldsymbol{\varepsilon}_i) = \sigma^2 \hat{d}_i^{2\delta}$, an exponential of the fitted value variance function, $\text{Var}(\boldsymbol{\varepsilon}_i) = \sigma^2 \exp(2\delta \hat{d}_i)$, or a constant plus power of the fitted value variance function, $\text{Var}(\boldsymbol{\varepsilon}_i) = \sigma^2(\delta_1 + \hat{d}_i^{\delta_2})^2$, where δ , δ_1 and δ_2 are estimated parameters (Pinheiro and Bates 2000). Among the three variance functions tested mentioned above, the exponential variance function demonstrated the best performance for the NLME single and variable-form taper models (see Appendix S and Table S3 in Supplementary Information for details for the performance comparison of NLME models with different variance functions). Thus, in this study we selected the exponential variance function to explain observed data heteroscedasticity.

Because the data used in the tree profile models were measured with an unequal distance along the stem, we used first-order autoregressive models [AR(1) models], first-order



continuous autoregressive correlation structure [CAR(1) models] and mixed autoregressive-moving average models (ARMA models) (Pinheiro and Bates 2000) to model the within-tree autoregressive structure of error and thus account for the autocorrelation of the data. Among the AR(1), CAR(1) and ARMA models, the CAR(1) model demonstrated the best performance for the NLME single and variable-form taper models (see Appendix S and Table S2 in Supplementary Information for details for the performance comparison of NLME models with different correlation structures). Thus, in this study we select the CAR(1) model to remove the autocorrelation of within the sample tree, which can be defined as $Cov(\varepsilon_{ij}, \varepsilon_{ij'}) = \rho^{d_{ij'}}$, where $Cov(\varepsilon_{ij}, \varepsilon_{ij'})$ is the covariance between two residuals ε_{ij} and $\varepsilon_{ij'}$ from tree i ; ρ is the estimated correlation parameter of first-order continuous autoregressive correlation structure [CAR(1)]; the continuous autoregressive error structure assumes that the within-sample tree correlation decreases with increase in distance $d_{ij'}$ between two observation h on tree i . $d_{ij'} = |h_{ij} - h_{ij'}|$, for $j \neq j'$ (Pinheiro and Bates 2000).

Prediction of diameter outside bark (d)

The prediction of d could be made by the NLME taper equation with or without random effects at tree level. The d prediction using NLME taper equation without random effects does not require prior diameter measurements from each tree. Only fixed-effects parameters were applied to predict the d mean response. Thus, the random-effects parameters (the expected value as 0) are not predicted. The d prediction using NLME taper equation with random effects requires prior measured diameter information. The mixed-effects parameters including both mean response (only fixed-effects parameters) and calibrated response (fixed- and random-effects parameters) were applied to predict subject-specific d calibrations. The empirical best linear unbiased prediction (EBLUP) method [Eq. (6)] (Vonesh and Chinchilli 1997) was used to calculate the sample tree-level random effects. The expression is written as Eq. (6)

$$\hat{\mathbf{u}}_i = \hat{\mathbf{D}}\hat{\mathbf{Z}}_i^T(\hat{\mathbf{R}}_i + \hat{\mathbf{Z}}_i\hat{\mathbf{D}}\hat{\mathbf{Z}}_i^T)^{-1}\hat{\mathbf{e}}_i \quad (6)$$

where $\hat{\mathbf{u}}_i$ is vector of the random effects from sample tree i ; $\hat{\mathbf{D}}$ is the estimated unstructured variance–covariance matrix for \mathbf{u}_i ; $\hat{\mathbf{R}}_i$ is the estimated matrix of within-tree variance–covariance for the error term; $\hat{\mathbf{e}}_i$ is the residuals vector, the components of which are calculated as the difference between the observed d value of the sample tree for the subsample and the predicted d value using the fixed-effects models; and $\hat{\mathbf{Z}}_i$ is the design matrix of the partial derivatives of Eq. (3), i.e., $\mathbf{Z}_i = \frac{\partial f(\beta, \mathbf{u}_i, \mathbf{X}_i)}{\partial \mathbf{u}_i} \Big|_{\hat{\beta}, \mathbf{u}_i=0}$.

The random-effects parameters of the NLME models were predicted using the method of random subsamples

(Sharma et al. 2016). A total of four randomly selected subsamples, which have low inventory cost and high prediction accuracy, have been recommended as the optimal sampling number for the most accurate calculation of the random-effects parameters, even when model types are different (Calama and Montero 2004; Fu et al. 2017b; Paulo et al. 2011). Thus, d measurements at four random h for each sample tree were used to predict the random effects of the tree profile model in this study. Details on the calculation of random-effects parameters for NLME models can be found in Meng and Huang (2009) and Fu et al. (2017b).

Model evaluation

As AIC and BIC can represent a penalized likelihood criteria, so they are widely used goodness-of-fit criteria for comparing taper models, where the dependent variable for each taper model was the same and all the models compared were fitted to the same data. In this study, in order to determine whether the fit and prediction performance of corresponding fixed- and mixed-effects models met the accuracy requirements, besides AIC and BIC, the following four statistical indicators for each model were calculated to determine the best stem taper model for *L. gmelinii*: adjusted coefficient of determination (R_{adj}^2), root mean squared error (RMSE), mean absolute error (MAB) and mean percentage of relative bias (MPRB).

Residual plots were generated to ensure satisfaction of the assumptions of normality and homoscedasticity of the residuals, identifying outliers when the standardized residuals of the observation value were lower than -2 or higher than $+2$ standard deviation (Dong et al. 2015; Feng 2004).

Results

Inclusion of AGE and P variables

There were significant differences in the relative diameter of the trees among the three P classifications (low, middle and high) along the entire tree stem ($0 < q \leq 1$; $F = 21.82$, $p < 0.001$; Table 2). The average relative diameter of tree bole in the stands with low P was 0.783 ± 0.003 , the biggest among all stands, significantly higher than the other two stands ($p < 0.001$, Table 2). Stands with different P showed different trends for relative diameter in each relative height (q intervals of 0.1). When q ranged from 0 to 0.1 and from 0.8 to 1.0, the relative diameter variables had no significant differences among stand densities, where tree boles are modeled geometrically in the forest literature commonly using neiloid and cone approaches, respectively. Relative diameter of the stands with low densities in q from 0.1 to 0.4 was

Table 2 ANOVA of relative diameter (mean ± standard error) for different stocking degrees (low, middle and high stocking degree) for different relative height classes (*q* intervals of 0.1)

Relative height	Low stocking degree		Middle stocking degree		High stocking degree		<i>F</i>	<i>p</i>
	<i>d/D</i>	<i>N</i>	<i>d/D</i>	<i>N</i>	<i>d/D</i>	<i>N</i>		
0 < <i>q</i> ≤ 1	0.783 ± 0.003 ^a	8719	0.763 ± 0.006 ^b	1460	0.713 ± 0.011 ^c	550	21.82	< 0.001
0 < <i>q</i> ≤ 0.1	1.044 ± 0.003 ^a	2288	1.032 ± 0.006 ^a	447	1.034 ± 0.009 ^a	143	2.24	0.106
0.1 < <i>q</i> ≤ 0.2	0.972 ± 0.002 ^a	912	0.915 ± 0.008 ^b	48	0.866 ± 0.006 ^c	51	132.34	< 0.001
0.2 < <i>q</i> ≤ 0.3	0.846 ± 0.002 ^a	1172	0.825 ± 0.003 ^b	228	0.806 ± 0.006 ^c	43	25.20	< 0.001
0.3 < <i>q</i> ≤ 0.4	0.803 ± 0.003 ^a	686	0.756 ± 0.005 ^b	98	0.732 ± 0.006 ^c	53	47.70	< 0.001
0.4 < <i>q</i> ≤ 0.5	0.713 ± 0.002 ^a	1124	0.688 ± 0.004 ^b	184	0.669 ± 0.006 ^{bc}	51	22.61	< 0.001
0.5 < <i>q</i> ≤ 0.6	0.636 ± 0.003 ^a	797	0.585 ± 0.004 ^b	196	0.590 ± 0.006 ^{bc}	59	51.31	< 0.001
0.6 < <i>q</i> ≤ 0.7	0.535 ± 0.003 ^a	664	0.517 ± 0.005 ^{ab}	121	0.496 ± 0.006 ^b	54	7.17	0.001
0.7 < <i>q</i> ≤ 0.8	0.441 ± 0.004 ^a	487	0.417 ± 0.010 ^{ab}	67	0.401 ± 0.007 ^b	54	7.30	0.001
0.8 < <i>q</i> ≤ 0.9	0.273 ± 0.005 ^a	357	0.278 ± 0.011 ^a	39	0.262 ± 0.014 ^a	26	0.22	0.804
0.9 < <i>q</i> < 1	0.136 ± 0.005 ^a	232	0.132 ± 0.013 ^a	32	0.136 ± 0.012 ^a	16	0.06	0.945

Superscript letters in the same row indicate significant differences between treatments (Tukey’s HSD, *p* < 0.05)

significantly different from the stands with the middle and high densities, reduced as the stand densities progressively increased, where a cylindrical shape was usually used to describe stem form. The section from the top end of the cylinder to the bottom start of the cone was characterized using a paraboloid, where *q* range is between 0.4 and 0.8, but the *q* range corresponding to different geometrical shapes is dependent on tree species. Differences in paraboloid stem form were not significant for stands with middle and high *P*.

The smallest relative diameter (0.717 ± 0.008) was found in the half-mature forest (Table 3). Differences in relative diameter among AGE classes were smaller than among *P*, but there were significant differences among young, half-mature and near-mature forests in relative diameter along the entire tree bole (0 < *q* ≤ 1) except for *q* from 0.7 to 1 (there were no differences between young and half-mature forests). In the *q* from 0.1 to 0.7, relative diameter in the mature forests was larger than over-mature forest and there were significant differences between the mature and over-mature forests (Table 3). However, in the *q* from 0 to 0.1 (neiloid) and 0.8 to 1.0 (cone) the relative diameter variables showed no significant differences between the mature and over-mature forests. In summary, ANOVA indicated that *P* and AGE exerted significant effects on the tree stem diameter.

Among all the models in which several functions of variables (all forms of AGE and *P*) were combined for the single [Eq. (1)] and variable-form [Eq. (2)] taper models, Eqs. (7) and (8), for which all the parameters were significant at the 95% confidence level, showed the lowest AIC (28,298.52 and 26,630.35) and BIC (28,333.81 and 26,715.04) values, and the largest logLik (−14,144.26 and −13,303.17) values, respectively. The final taper equations including AGE and *P* information were written as

Newberry and Burkhart (1986) model with AGE and *P*:

$$d_{ij} = \left\{ [b_1 + b_2 \ln(\text{AGE}_i)] \left(\frac{H_i - h_{ij}}{H_i - 1.3} \right)^{(b_3 + b_4 \sqrt{P_i})} \right\} D_i + \epsilon_{ij} \tag{7}$$

Kozak (2004)-(2) model with AGE and *P*:

$$d_{ij} = b_1 D_i^{b_2} H_i^{b_3} x_{ij}^{b_4} \left[b_5 q_{ij}^{b_5} + b_6 [1/e^{D_i/H_i}] + b_6 x_{ij}^{b_6} + b_7 (1/D_i) + b_8 H_i^{(1-q_{ij}^{1/3})} + b_9 x_{ij} + b_{10} \text{AGE}_i + b_{11} P_i \right] + \epsilon_{ij} \tag{8}$$

where AGE_{*i*} and P_{*i*} are age of the *i*th tree and the stocking degree of the stand in which the *i*th tree is located, respectively, and b₁–b₁₁ are model parameters.

The parameters, which were significant at the 95% confidence level, in the models adding the AGE and *P* [Eqs. (7) and (8)] for the single and variable-form taper models are shown in Table 4.

NLME models and parameter estimates

When considering sample tree-level random effects, Eq. (7) with more than three random-effects parameters and Eq. (8) with more than two random-effects parameters failed to reach convergence (the different tolerances of the two adjacent iterations are more than 0.000001, with a maximum number of iterations of 50). Preliminary analysis showed that Eqs. (7) and (8) including two random-effects parameters were better than Eqs. (7) and (8) including one random-effects parameter among the converged mixed-effects



Table 3 ANOVA of relative diameter (mean ± standard error) for different tree age classes (young, half-mature, near-mature, mature and over-mature forests) for different relative height classes (*q* intervals of 0.1)

Relative height	Young forest		Half-mature forest		Near-mature forest		Mature forest		Over-mature forest		<i>F</i>	<i>p</i>
	<i>d</i> / <i>D</i>	<i>N</i>	<i>d</i> / <i>D</i>	<i>N</i>	<i>d</i> / <i>D</i>	<i>N</i>	<i>d</i> / <i>D</i>	<i>N</i>	<i>d</i> / <i>D</i>	<i>N</i>		
0 < <i>q</i> ≤ 1	0.786 ± 0.003 ^a	7429	0.717 ± 0.008 ^b	1368	0.785 ± 0.009 ^a	1238	0.777 ± 0.201 ^a	291	0.769 ± 0.017 ^a	403	21.71	< 0.001
0 < <i>q</i> ≤ 0.1	1.006 ± 0.001 ^a	2174	1.103 ± 0.010 ^b	279	1.208 ± 0.014 ^c	239	1.162 ± 0.024 ^d	73	1.148 ± 0.019 ^d	111	287.58	< 0.001
0.1 < <i>q</i> ≤ 0.2	0.969 ± 0.002 ^a	646	0.942 ± 0.006 ^b	144	0.975 ± 0.003 ^a	152	0.956 ± 0.009 ^{ab}	34	0.913 ± 0.008 ^c	35	16.59	< 0.001
0.2 < <i>q</i> ≤ 0.3	0.833 ± 0.001 ^a	1171	0.865 ± 0.006 ^b	116	0.901 ± 0.004 ^c	99	0.885 ± 0.012 ^{bcd}	20	0.850 ± 0.010 ^{ab}	37	54.62	< 0.001
0.3 < <i>q</i> ≤ 0.4	0.777 ± 0.003 ^a	536	0.794 ± 0.007 ^b	122	0.849 ± 0.004 ^c	125	0.852 ± 0.013 ^{cd}	23	0.792 ± 0.010 ^{ab}	31	39.73	< 0.001
0.4 < <i>q</i> ≤ 0.5	0.696 ± 0.002 ^a	1054	0.721 ± 0.006 ^b	131	0.781 ± 0.005 ^c	113	0.787 ± 0.010 ^{cd}	25	0.732 ± 0.012 ^{bc}	36	75.30	< 0.001
0.5 < <i>q</i> ≤ 0.6	0.604 ± 0.002 ^a	745	0.640 ± 0.007 ^b	138	0.715 ± 0.006 ^c	109	0.699 ± 0.016 ^{cd}	24	0.651 ± 0.011 ^{bc}	36	91.88	< 0.001
0.6 < <i>q</i> ≤ 0.7	0.504 ± 0.003 ^a	537	0.528 ± 0.006 ^b	124	0.621 ± 0.008 ^c	121	0.605 ± 0.018 ^{cd}	22	0.566 ± 0.013 ^{de}	35	78.00	< 0.001
0.7 < <i>q</i> ≤ 0.8	0.421 ± 0.004 ^a	313	0.408 ± 0.007 ^{ab}	134	0.492 ± 0.010 ^c	108	0.464 ± 0.020 ^{ac}	25	0.470 ± 0.016 ^c	30	21.96	< 0.001
0.8 < <i>q</i> ≤ 0.9	0.255 ± 0.007 ^a	148	0.247 ± 0.007 ^a	116	0.315 ± 0.010 ^b	107	0.286 ± 0.020 ^{ab}	27	0.297 ± 0.021 ^{ab}	24	10.38	< 0.001
0.9 < <i>q</i> ≤ 1	0.123 ± 0.006 ^a	105	0.137 ± 0.008 ^{ab}	64	0.162 ± 0.011 ^b	65	0.127 ± 0.017 ^{ab}	18	0.126 ± 0.015 ^{ab}	28	3.17	0.014

Superscript letters in the same row indicate significant differences between treatments (Tukey's HSD, *p* < 0.05)

models. The best two random-effects parameters for Eqs. (7) and (8) were associated with the parameters *b*₂ and *b*₄, and *b*₁ and *b*₆, respectively. The following Eqs. (9) and (10) had the lowest AIC (27,236.59 and 25,349.94) and BIC (27,293.05 and 25,455.80) values, and the highest logLik (−13,610.30 and −12,659.97) values. In addition, all the parameters of Eqs. (9) and (10) were significant at the 95% confidence level, and Eqs. (9) and (10) were thus selected as the optimal NLME single and variable-form taper models, respectively:

$$d_{ij} = \left\{ [b_1 + (b_2 + u_{2i}) \ln(\text{AGE}_{ij})] \left(\frac{H_i - h_{ij}}{H_i - 1.3} \right)^{(b_3 + (b_4 + u_{4i}) \sqrt{P_i})} \right\} D_i + \varepsilon_{ij} \tag{9}$$

$$d_{ij} = (b_1 + u_{1i}) D_i^{b_2} H_i^{b_3} \left[x_{ij}^{b_4} + b_5 [1/e^{D_i/H_i}] + (b_6 + u_{6i}) x_{ij}^{b_1} + b_7 (1/D_i) + b_8 H_i^{(1-q_{ij}^{1/3})} + b_9 x_{ij} + b_{10} \text{AGE}_i + b_{11} P_i \right] + \varepsilon_{ij} \tag{10}$$

where *u*_{2*i*}, *u*_{4*i*}, *u*_{1*i*} and *u*_{6*i*} are the random-effects parameters produced by the *i*th sample tree on *b*₂, *b*₄, *b*₁ and *b*₆, respectively.

Equations (9) and (10) including each of the three variance functions and the three correlation structures significantly improved model performance (using L.Ratio, *p* < 0.0001) comparing with the models in which homogeneous variances were assumed (Table S2 and S3). Even with random effects in the parameters, heteroscedasticity and autocorrelation persisted in the NLME single and variable-form taper models [Eqs. (9) and (10)]. Consequently, both Eqs. (9) and (10) were fitted with exponential variance functions and CAR(1) with the best performance to further explain the variance heterogeneity and autocorrelation, respectively. The parameters, which were significant at the 95% confidence level, in the complete NLME models of *L. gmelinii* (the foundation models adding the AGE and *P* at sample tree level combining exponential variance function and CAR(1) model) for the single and variable-form taper profile models were estimated as follows [Eqs. (11) and (12)]. Equations (11) and (12) had lower AIC (23,025.68 and 22,467.98) and BIC (23,096.26 and 22,587.96) values, and larger logLik (−11,502.84 and −11,216.99) values than Eqs. (9) and (10).

Table 4 Regression coefficients and standard errors (in parentheses) for Newberry and Burkhart (1986) model and Kozak (2004)-(2) model without (Eqs. (1) and (2)) and with (Eqs. (7) and (8)) tree age (AGE) and stocking degree (P)

Model	b1	b2	b3	b4	b5	b6	b7	b8	b9	b10	b11
Equation (1)	1.0065 (0.0011)	0.7265 (0.0029)									
Equation (2)	0.9687 (0.0084)	0.9759 (0.0053)	0.0445 (0.0074)	7.0916 (0.1319)	-1.1192 (0.2323)	-10.4929 (0.3488)	-0.6966 (0.0506)	0.0163 (0.0036)	15.1469 (0.4142)		
Equation (7)	0.9141 (0.0031)	0.0293 (0.0009)	0.3793 (0.0205)	0.4043 (0.0234)							
Equation (8)	0.9731 (0.0082)	0.9749 (0.0051)	0.0441 (0.0072)	7.4220 (0.1299)	-0.2243 (0.2532)	-11.6700 (0.3683)	-1.9030 (1.0140)	0.0123 (0.0035)	15.8800 (0.4072)	-0.0036 (0.0002)	0.6589 (0.0944)

The complete NLME single taper profile model:

$$\left\{ \begin{array}{l}
 d_{ij} = \{ [0.8832452 + (0.0462792 + u_{2i}) \ln(\text{AGE}_i)] \left(\frac{H_i - h_{ij}}{H_i - 1.3} \right)^{(0.4656135 + (0.3236165 + u_{4i}) \sqrt{P_i})} \} D_i + \varepsilon_{ij} \\
 \mathbf{u}_i = \begin{bmatrix} u_{2i} \\ u_{4i} \end{bmatrix} \sim N \left\{ \begin{bmatrix} 0 \\ 0 \end{bmatrix}, \begin{pmatrix} 0.000013 & 0.000105 \\ 0.000105 & 0.010380 \end{pmatrix} \right\} \\
 \varepsilon_i \sim N(0, \mathbf{R}_i), \mathbf{R}_i = 0.466672 \mathbf{G}_i^{0.5} \mathbf{\Gamma}_i \mathbf{G}_i^{0.5} \\
 \mathbf{G}_i = \text{diag}(\exp(2 \times 0.04982316 d_{i1}), \dots, \exp(2 \times 0.04982316 d_{in_i})) \\
 \mathbf{\Gamma}_i \sim \text{CAR}(1) = \begin{pmatrix} 1 & 0.3349^{d_{12}} & \dots & 0.3349^{d_{1n_i}} \\ 0.3349^{d_{12}} & 1 & \dots & 0.3349^{d_{2n_i}} \\ \vdots & \vdots & \ddots & \vdots \\ 0.3349^{d_{1n_i}} & 0.3349^{d_{2n_i}} & \dots & 1 \end{pmatrix}
 \end{array} \right. \tag{11}$$

The complete NLME variable-form taper profile model:

$$\left\{ \begin{array}{l}
 d_{ij} = (1.00049 + u_{1i}) D_i^{0.94522} H_i^{0.06256} x_{ij} \left[6.88847 d_{ij}^4 - 2.06853 [1/e^{D_i/H_i}] + (-7.49948 + u_{6i}) x_{ij}^{0.1} + 2.44390 (1/D_i) + 0.02319 H_i^{(1-d_{ij}^{1/3})} + 11.72306 x_{ij} - 0.00690 \text{AGE}_i + 0.37088 P_i \right] + \varepsilon_{ij} \\
 \mathbf{u}_i = \begin{bmatrix} u_{1i} \\ u_{6i} \end{bmatrix} \sim N \left\{ \begin{bmatrix} 0 \\ 0 \end{bmatrix}, \begin{pmatrix} 0.000242 & 0.004351 \\ 0.004351 & 0.156640 \end{pmatrix} \right\} \\
 \varepsilon_i \sim N(0, \mathbf{R}_i), \mathbf{R}_i = 0.456472 \mathbf{G}_i^{0.5} \mathbf{\Gamma}_i \mathbf{G}_i^{0.5} \\
 \mathbf{G}_i = \text{diag}(\exp(2 \times 0.04927 d_{i1}), \dots, \exp(2 \times 0.04927 d_{in_i})) \\
 \mathbf{\Gamma}_i \sim \text{CAR}(1) = \begin{pmatrix} 1 & 0.3306^{d_{12}} & \dots & 0.3306^{d_{1n_i}} \\ 0.3306^{d_{12}} & 1 & \dots & 0.3306^{d_{2n_i}} \\ \vdots & \vdots & \ddots & \vdots \\ 0.3306^{d_{1n_i}} & 0.3306^{d_{2n_i}} & \dots & 1 \end{pmatrix}
 \end{array} \right. \tag{12}$$

Evaluation of model fitting and validation

Four randomly selected diameters for each sampled tree were used to calculate the random effects of the tree profile NLME models in this study. Table 5 summaries the evaluation indices of the fitting and validation for fixed and NLME models of single and variable-form taper models based on the fitting and validation datasets.

All six models showed acceptable goodness of fit and validation, accounting for more than 97% of *L. gmelinii* taper

variation (Table 5). Regardless of the fitting or validation data, each variable-form taper profile model (except for the Kozak (2004)-(2) model) showed a better performance than the single taper profile model. The MAB and MPRB of the validation data for the Kozak (2004)-(2) model were much larger than those of the NLME model combining CAR(1) and an exponential variance function for the single taper profile model [Eq. (11)]. Of the single taper profile models, Eq. (11) performed best, followed by the foundation



Table 5 Evaluation statistics of NLME models and models with and without tree age (AGE) and stocking degree (P) for the Newberry and Burkhart (1986) and Kozak (2004)-(2) models

Model No.	Fitting							Validating		
	R^2_{adj}	RMSE	MAB	MPRB (%)	AIC	BIC	logLik	RMSE	MAB	MPRB (%)
Single taper models										
Equation (11)	0.97951	1.15163	0.67737	5.13700	23,025.7	23,096.3	-11,502.8	1.03868	0.64442	4.88682
Equation (7)	0.97557	1.25764	0.72778	5.51927	28,298.5	28,333.8	-14,144.3	1.12334	0.69834	5.29571
Equation (1)	0.97234	1.33797	0.74581	5.65600	29,359.4	29,380.6	-14,676.7	1.17807	0.70600	5.35382
Variable-form taper models										
Equation (12)	0.98250	1.06436	0.64142	4.86440	22,468.0	22,588.0	-11,217.0	0.94898	0.61193	4.64041
Equation (8)	0.98135	1.09917	0.67059	5.08559	26,630.4	26,715.0	-13,303.2	0.96067	0.63149	4.78873
Equation (2)	0.98165	1.08979	0.66981	5.07970	27,014.5	27,085.1	-13,497.3	0.99333	0.65384	4.95823

model incorporating AGE and P variables [Eq. (7)] and then by the foundation model [Eq. (1)], which showed an average RMSE decrease of 13.93% and 11.83% for fitting and validation, respectively. There were also corresponding decreases of 9.18% and 8.72% in MAB and MPRB for fitting and validation, respectively. Similarly, in the variable-form taper profile models, NLME model combining CAR(1) and exponential variance function [Eq. (12)] had the smallest RMSE, MAB and MPRB. Models adding AGE and P [Eq. (8)] showed slightly worse performance in the fitting statistics than the foundation model [Eq. (2)], but better validation statistics (Table 5). However, Eq. (8) demonstrated lower AIC ($26,630.35 < 27,014.52$) and BIC ($26,715.04 < 27,085.09$) values, and larger logLik values ($-13,303.17 > -13,497.26$) for predicting the stem diameter of any tree height. The RMSE decrease ranged from 2.39 to 4.67%, and the MAB and MPRB decrease ranged from 4.43 to 6.86%, depending on whether the fitting or validation dataset was applied. Based on AIC, BIC, logLik, and fitting and validation statistics, the NLME models including the exponential variance function and CAR(1) eliminated

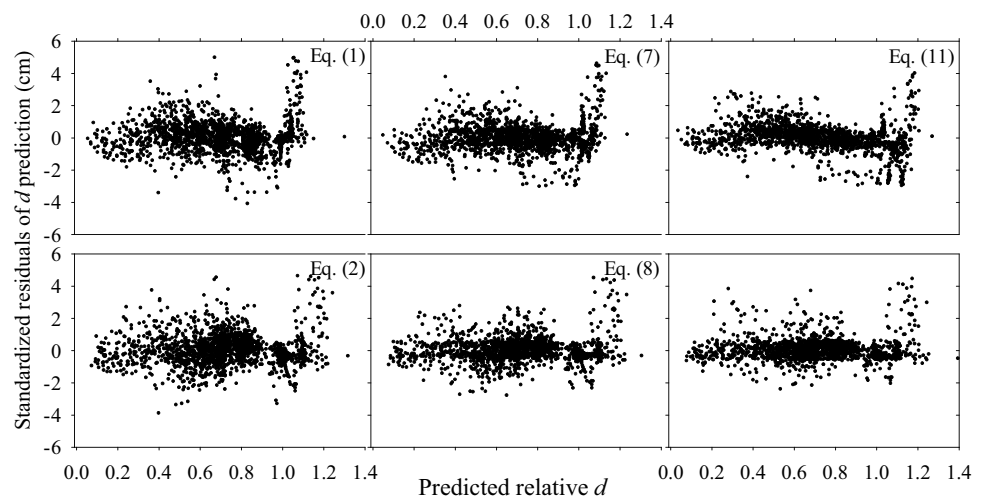
the heteroscedasticity and autocorrelation and significantly improved the predicted performance.

The standardized residual plots also showed that residuals of all six models were distributed around the zero mean, except the bottom sections of the stem, which were substantially larger than ± 2 standard deviation (Fig. 2, $1.0 < \text{predicted relative } d \leq 1.2$). It is clear that residual variance of Eq. (12) was more homogeneous along the tree bole and Eq. (1) showed a much poorer performance than other models (Fig. 2). Overall, based on the fitting and validation indicators and standardized residual plots, Eq. (12) was identified as the optimal model for modeling taper profile of *L. gmelinii* in the Greater Khingan Mountains of Inner Mongolia, northeast China.

An example application of the developed single and variable-form taper models

Figure 3 shows the simulation of diameters at corresponding heights along the tree bole for a selected tree of *L. gmelinii*

Fig. 2 Diameter outside bark residuals plotted against predicted relative d for Newberry and Burkhart (1986) and Kozak (2004)-(2) models fitted only without tree age (AGE) and stocking degree (P) incorporated [Eqs. (1) and (2)], with AGE and P incorporated [Eqs. (7) and (8)], and with fixed- and random-effects parameters (with AGE and P incorporated) plus an autoregressive error structure CAR(1) and exponential variance function [Eqs. (11) and (12)]



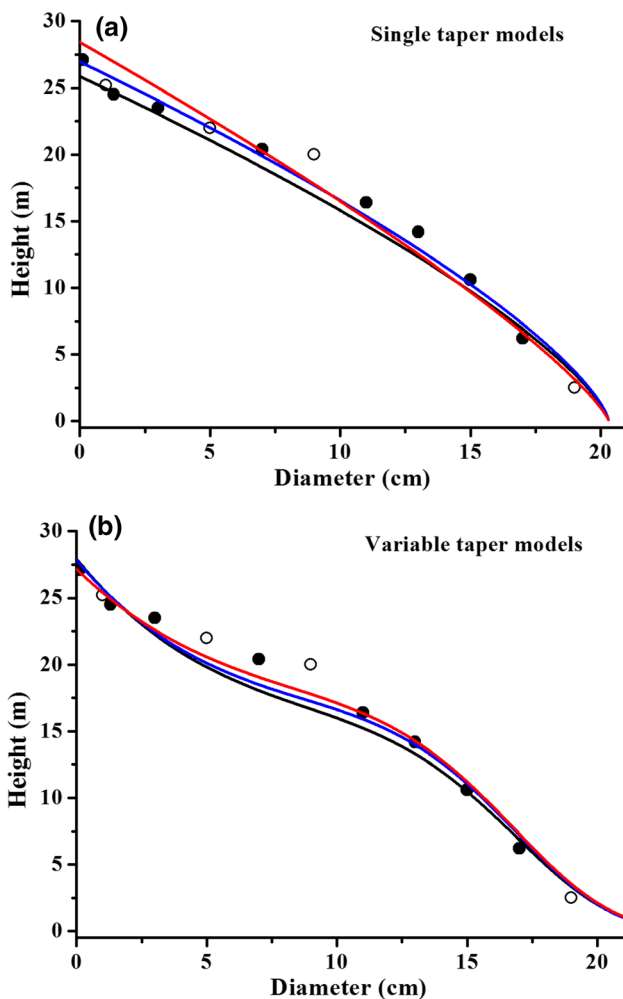


Fig. 3 An example stem profile simulation using the Newberry and Burkhardt (1986) and Kozak (2004)-(2) models (black lines), Newberry and Burkhardt (1986) and Kozak (2004)-(2) models with tree age (AGE) and stocking degree (P) (blue lines), and Newberry and Burkhardt (1986) and Kozak (2004)-(2) models with AGE and P and with fixed- and random-effects parameters plus CAR(1) and an exponential variance function (red lines). The calibrated response of NLME models (Newberry and Burkhardt (1986) and Kozak (2004)-(2) models with AGE and P and with fixed- and random-effects parameters plus CAR(1) and an exponential variance function) was based on four randomly selected upper-stem diameters at $h = 1.0, 5.0, 9.0$ and 19.0 m for the same sample tree ($D = 24.5$ cm, $H = 20.3$ m, AGE = 103 years and $P = 0.71$). The three color codes represent the three different models of single and variable-form taper models. The dots represent the measured value of the upper-stem diameter at corresponding height along the tree bole. The stem diameters used for calibration are represented by four hollow dots

($D = 24.5$ cm, $H = 20.3$ m, AGE = 103 years and $P = 0.71$, from the validation dataset).

(1) If tree age, stocking degree and four random complementary upper-stem diameter measurements are available ($h = 1.0, 5.0, 9.0$ and 19.0 m and $d = 25.2, 22.0, 20.0$ and 2.5 cm at the corresponding height h) for this selected tree, the vector of the random-effects parameters $\hat{\mathbf{u}}_i$ for the

NLME single and variable-form taper models can be estimated using the EBLUP [Eq. (6)]:

$$\mathbf{u}_{i(s)} = \begin{bmatrix} u_{2i} \\ u_{4i} \end{bmatrix} = \begin{bmatrix} 0.00059 \\ 0.07566 \end{bmatrix} \text{ for the NLME single taper}$$

model, and $\mathbf{u}_{i(v)} = \begin{bmatrix} u_{1i} \\ u_{6i} \end{bmatrix} = \begin{bmatrix} 0.00358 \\ 0.02753 \end{bmatrix}$ for the NLME variable-form taper model. Then, the random-effects parameter values $\hat{\mathbf{u}}_i$ were substituted into Eqs. (11) and (12) to obtain the tree-specific stem diameters at the corresponding height (Fig. 3, red lines);

(2) If tree age and stand stocking are available but no stem diameter measurement is available, then Eqs. (11) or (12) are still the equations used to obtain the mean upper-stem diameter prediction only using the fixed parameter estimates as the random effects can no longer be predicted and the random-effects vectors were assumed to be equal to their expected estimates $E(\mathbf{u}_i = 0)$;

(3) If tree age and stocking degree are not available and only D and H are known, strictly speaking, Eqs. (1) and (2) are still invalid to estimate the stem diameters if they were fitted using nonlinear least squares and there is heteroscedasticity and autocorrelation in residuals. But if the requirement to model accuracy is not very high and the error is acceptable, Eqs. (1) and (2) can be used to estimate the stem diameters at the corresponding height (Fig. 3, black lines). Because model parameters estimated using nonlinear least squares are still unbiased, only estimated variances and confidence interval estimation on model parameters are biased (the parameters of Eqs. (1) and (2) can be found in Table 4). If we also know AGE and P , similarly, Eqs. (7) and (8) can be used to estimate the stem diameters at the corresponding height (Fig. 3, blue lines). Overall, the NLME taper models including both fixed-effects parameters and calibrated responses improved the model d prediction, particularly in the middle and near the top of the stem, where bias of d was the lowest (Fig. 3).

Discussion

Stem taper foundation models for *L. gmelinii*

This study identified the optimal stem taper foundation models on the basis of the statistical indicators and model simplicity as the Newberry and Burkhardt (1986) and Kozak (2004)-(2) models for the single and variable-form taper models. However, our results were not fully consistent with previous studies. Adding to this inconsistency among previous studies, Sakici et al. (2008) recommended the Demaerschalk (1972) model as the optimal single taper model for Bornmullerian fir (*Abies nordmanniana* subsp.

bornmulleriana Mattf.), which was the most accurate single taper model for the selected 17 simple polynomial in their study. Yet Rojo et al. (2005) found that the single taper functions developed by Cervera (1973) provided the most accurate predictions among 19 other single taper models for maritime pine (*Pinus pinaster* Ait.). One of the main reasons for such disparity of results is the simple ecophysiological fact that there is no general stem taper model to provide a better description for all tree species, as different tree species have different wood properties, growth rates, and aboveground architecture. To make things more complicated, all these factors have strong genetic and site-specific environmental drivers.

In the present study, the Kozak (2004)-(2) variable-form taper model showed the best performance for *L. gmelinii*, agreeing with results by Kozak (2004) who concluded it was the best taper model to estimate diameter inside bark and suggested that it could be widely applied to many tree species. Supporting the transferability of this model, the Kozak (2004)-(2) variable-form taper model similarly provided the best performance in describing the stem profile of five major pine species in El Salto (Durango, Mexico) (Corral-Rivas et al. 2007); lodgepole pine (*Pinus contorta* var. *latifolia* Engelm.) (Yang et al. 2009b); birch (*Betula pubescens* Ehrh.) (Gómez-García et al. 2013); and red spruce (*Picea rubens* (Sarg.)) and white pine (*Pinus strobus* (L.)) (Li and Weiskittel 2010). Menéndez-Miguélez et al. (2014) also described superior performance using the Kozak (2004)-(2) model in predicting diameter for chestnut (*Castanea sativa* Mill.) coppiced stands.

However, despite such reports on superior performance, the Kozak (2004)-(2) taper model still has relatively large residuals at the tree stem butt (Fig. 2) and is a non-compatible variable-exponent taper model. One reason could be the lack of clear ecophysiological parameters in a purely mathematical model, as many of the early taper models have been developed using data from even-age secondary forests or even plantations, in which growth variability among trees is reduced compared to a natural dense forest. When including age and tree density, some of the variability in micro-site and tree conditions directly affecting growth conditions of each individual tree is therefore taken into account, improving predictions of stem taper, as seen in Fig. 3.

In general, it is assumed that the variable-form taper model had the lowest bias when estimating diameters along the tree bole, closely followed by the segmented and single taper models (Rojo et al. 2005; Sakici et al. 2008). However, our results do not support this assumption, as they indicated that the single taper model by Newberry and Burkhart (1986) provided more accurate prediction than the Max and Burkhart (1976) segmented taper model. Similarly, Özçelik and Crecente-Campo (2016) found that variable-form taper models were inferior to segmented taper models in terms

of prediction accuracy, which is again in contradiction with the most common results described in the literature. Given these inconsistencies among studies, it is clear that no optimal taper model (either single or variable-form) exists and that species- and site-specific factors are influential in stem shape.

Modeling AGE and *P* effects on taper of *L. gmelinii*

Some previous studies suggested that predictors of *h*, *H* and DBH were able to accurately model the stem taper, while other studies considered that including predictors of tree age (Muhairwe et al. 1994; Tasissa and Burkhart 1998), stand density (Muhairwe et al. 1994; Scolforo et al. 2018; Sharma and Parton 2009) and climatic variables (Schneider 2018) would best improve the stem taper prediction accuracy. However, based on our results, we argue that stem taper models including *h*, *H* and DBH as the independent variables may be sufficiently accurate for even aged stands and stands with a consistent density, but might not be so for natural forests, supporting our first hypothesis.

The corroboration of our first hypothesis is sustained by the significant improvements observed for the stem taper model incorporating AGE and *P* as predictor variables. For example, the predictive ability on the upper stem for the Kozak (2004)-(2) taper model with AGE and *P* was higher than without AGE and *P* (Fig. 2). This could be because the Kozak (2004)-(2) model incorporating AGE and *P* had greater biological relevance than the foundation model. The effect of AGE on stem taper is likely to be mostly associated with the tree crown as the upper stem receives more sunlight than the lower stem (Barnes et al. 1998) and the tree crown responds to changes in stand density (*P*). Previous studies have also shown that the addition of new parameters substantially improved stem form predictions. For example, the introduction of crown class, site class and breast height age into the Kozak (1988) variable-exponent taper model (Muhairwe et al. 1994); total basal area (BA) and *D*, i.e., (\sqrt{BA}/D) into the Sharma and Oderwald (2001) model (Sharma and Parton 2009); or slenderness (reflected by height to diameter ratio) and crown base height into a variable-exponent model (Courbet and Houllier 2002), all improved the basic model's accuracies.

However, in our results the prediction accuracy for stem taper models with AGE and *P* was still low in the neiloid shape (Fig. 2, $1.0 < \text{predicted relative } d \leq 1.2$), for which there was no significant difference between models with and without AGE and *P* as independent variables. There are three possible reasons for this result. First, *P* had no effect and AGE had little to no effect (between mature and over-mature forests) on the relative diameters for the frustum of the neiloid ($0 < q \leq 0.1$, Table 2, 3). Second, a neiloid taper equation is especially adequate to model stump volume, but

if stump diameter has been used to estimate DBH, error is introduced when estimating volume from DBH (Pond and Froese 2014). Third, although tree growth primarily follows biological limitations, stem growth depends on complex multifactorial and site-specific factor combinations, which are complicated and thus hard to model with statistical methods. Empirical and theoretical taper equations only simulate the effect of relative height change on taper. No matter how accurate the equation, uncertainty cannot be completely eliminated, because all models are simplifications of reality (Kimmins et al. 2008).

Mixed-effects taper models for *L. gmelinii*

Our results demonstrated that incorporating two random-effects parameters led to more accurate predictions of stem taper, supporting our second hypothesis. Such result indicate that accounting for the sampled tree as a random effect accounted for part of the variability and therefore the result was a more reliable prediction of diameters along the tree stem. It is crucial for studies applying mixed-effects models to determine the within-tree variance–covariance structure for the matrix of the error term \mathbf{R}_i . Both the NLME single taper model [Eq. (11)] and NLME variable-form taper model [Eq. (12)] used exponential variance functions and CAR(1) to minimize the effect for the within-tree heteroscedasticity and autoregressive structure of error, respectively. In this manner, Eqs. (11) and (12) improved the model performances relative to other NLME model forms that did not include CAR(1) and exponential variance functions [Eqs. (9) and (10), Table S2 and S3] or fixed-effects models of the stem profile (Table 5, Fig. 2). Other authors have also shown that adding CAR(1) to the taper model greatly removed the autocorrelation (Li and Weiskittel 2010; Trincado and Burkhart 2006; Younger 2007). In addition, an exponential variance function had a better correction effect on the heterogeneous residual variances than a power variance function for repeated-measures data (Fu et al. 2017a; Trincado and Burkhart 2006; Zhao et al. 2005). However, some studies have shown that heterogeneous residual variances could be corrected by weighting through a power variance function (Wang et al. 2014; Yang et al. 2009a).

One of the earliest examples of the inclusion of random effects in forestry applications was the generation of height growth curves (Lappi and Bailey 1988). In the same line as our results, NLME models have been successfully applied to the development of taper equations (Özçelik et al. 2011), crown width equations (Fu et al. 2013; Yang and Huang 2017), biomass equations (Njana et al. 2016), tree height and diameter equations (Gollob et al. 2018; MacPhee et al. 2018; Mehtätalo et al. 2015) and top height equations (Sharma and Reid 2018). This suggests that the inclusion of random-effects parameters significantly improves the fit of

the corresponding equations by capturing part of the natural variability related to biological processes involved in tree growth.

Estimation of the random-effects parameters of the NLME model is a key step in model applications based on the EBLUP method [Eq. (6)] and explicit derivation of corresponding models if additional diameter subsamples are available. NLME models significantly improved their predictive ability relative to the fixed-effects models with reduction of RMSE by 1.22–13.93% and R_{adj}^2 increase of 0.09–0.74% (Table 5), based on the calibrated response using four random measured upper-stem diameters for each sample tree. Hence, our results with previous research suggesting four as the optimal subsample size used in estimating random effects (Calama and Montero 2004; Fu et al. 2017a; Paulo et al. 2011).

Although models fitted considering random-effects parameters can eliminate the autocorrelation and heteroscedasticity, a compromise should be achieved between model prediction accuracy requirements for practical applications, complexity of the error covariance structure when using more than one randomly selected subsample, and operational costs involved in additional diameter measurements to estimate random-effects parameters. It is difficult to estimate the random effects within sample trees unless four randomly selected diameters at different points along the same tree stem are available for the calibration of the NLME models. However, recent advances in measurement equipments make this issue of accurately measuring four upper-stem diameter measurements on standing trees in a forested setting less problematic. In addition, sometimes the reduction of the precision of the models by measurement error exceeds the improvement in precision from the inclusion of the random-effects parameters (Fu et al. 2017b; Gómez-García et al. 2013). This could arise in the following cases: (1) deformed diameter measurement, such as forked, sunken or burl stems or trees lacking apical dominance; (2) the field measurement errors encountered by field staff or faulty instruments (Fu et al. 2017b; Omule 1980); or (3) the choice of number of diameter classes (Schröder et al. 2015), and the values of AGE and P .

Our results show the viability of including more ecologically meaningful parameters (such as tree age and stocking degree) but at the same time improving accuracy of taper equations, reaching therefore a more adequate degree of model complexity (Kimmins et al. 2008). Such enhanced models can be used to improve estimations of volume, biomass or carbon in standing forests as well as in harvested trees.

Conclusions

Out of the 30 stem taper foundation models studied, the Newberry and Burkhart (1986), Max and Burkhart (1976) and Kozak (2004)-(2) models showed the best estimates for diameters along the stem. Of these, the Max and Burkhart (1976) model provided the worst accurate predictions. As we hypothesized, AGE and P exhibited significant effects on tree stem and improved the models when incorporated into the taper equations. As we also hypothesized, common exponential variance functions and CAR(1) can be used to minimize within-tree heteroscedasticity and autoregressive structure of error for both NLME models. The NLME taper models included both fixed-effects parameters and calibrated responses when four random complementary upper-stem diameter measurements are available for a new tree, which improved the fitting and predicting abilities of model estimation for diameter at any height along the tree bole. We have then provided the first improved taper modes with NLME single and variable-form taper models for natural forests of *L. gmelinii* in the Greater Khingan Mountains of Inner Mongolia, northeast China [Eqs. (11) and (12)], but our approach is probably suitable for other tree species, and the example provided here can be used as guidance for further research.

In conclusion, when developing taper functions for trees in natural forests it is strongly suggested that tree age and stocking degree to be accounted for in the model, and if possible, the introduction of a random-effects model to account for the potential violation of assumptions in the stem data used to create the models. These recommendations are timely and relevant as the need for accurate timber volume estimation in multi-aged, dense stands is already increasing as forest management moves toward management regimes closer to nature, precisely by increasing the number of tree age cohorts in secondary forests, therefore making them more similar to natural forests such as those used in this research.

Acknowledgements We thank Professor Qibao Zhang from Inner Mongolia Agricultural University for providing to the data used in this analysis. We would also like to thank all anonymous reviewers. This study was funded by the National Key R&D Program of China (2017YFC0504003-2), National Natural Science Foundations of Inner Mongolia Autonomous Region (2015BS0303) and Excellent Young Scientist Foundation of Inner Mongolia Agricultural University of China (No. 2014XYQ-6).

References

- Agriculture and Forestry Planning Team of Inner Mongolia Autonomous Region (1974) Forest inventory table. Publisher unknown, Hohhot
- Barnes BV, Zak DR, Denton SR, Spurr SH (1998) Forest ecology, 4th edn. Wiley, New York
- Bi H (2000) Trigonometric variable-form taper equations for Australian eucalypts. For Sci 46:397–409. <https://doi.org/10.1093/forestscience/46.3.397>
- Bi H, Long Y (2001) Flexible taper equation for site-specific management of *Pinus radiata* in New South Wales, Australia. For Ecol Manag 148:79–91. [https://doi.org/10.1016/S0378-1127\(00\)00526-0](https://doi.org/10.1016/S0378-1127(00)00526-0)
- Bitterlich W (1984) The relascope idea. Relative measurements in forestry. Commonwealth Agricultural Bureaux, Slough
- Brooks JR, Jiang L, Özçelik R (2008) Compatible stem volume and taper equations for Brutian pine, Cedar of Lebanon, and Cilicica fir in Turkey. For Ecol Manag 256:147–151. <https://doi.org/10.1016/j.foreco.2008.04.018>
- Burkhart HE, Walton SB (1985) Incorporating crown ratio into taper equations for loblolly pine trees. For Sci 31:478–484. <https://doi.org/10.1093/forestscience/31.2.478>
- Calama R, Montero G (2004) Interregional nonlinear height-diameter model with random coefficients for stone pine in Spain. Can J For Res 34:150–163. <https://doi.org/10.1139/x03-199>
- Calama R, Montero G (2005) Multilevel linear mixed model for tree diameter increment in stone pine (*Pinus pinea*): a calibrating approach. Silva Fenn 39:37–54
- Calama R, Montero G (2006) Stand and tree-level variability on stem form and tree volume in *Pinus pinea* L.: a multilevel random components approach. For Syst 15:24–41. <https://doi.org/10.5424/srf/2006151-00951>
- Cervera J (1973) El área basimétrica reducida, el volumen reducido y el perfil. Montes 174:415–418
- Clutter JL, Fortson JC, Pienaar LV, Brister GH, Bailey RL (1983) Timber management: a quantitative approach. Wiley, New York
- Corral-Rivas JJ, Diéguez-Aranda U, Corral Rivas S, Castedo Dorado F (2007) A merchantable volume system for major pine species in El Salto, Durango (Mexico). For Ecol Manag 238:118–129. <https://doi.org/10.1016/j.foreco.2006.09.074>
- Courbet F, Houllier F (2002) Modelling the profile and internal structure of tree stem. Application to *Cedrus atlantica* (Manetti). Ann For Sci 59:63–80. <https://doi.org/10.1051/forest:2001006>
- Demaerschalk JP (1972) Converting volume equations to compatible taper equations. For Sci 18:241–245. <https://doi.org/10.1093/forestscience/18.3.241>
- Development Core Team R (2017) R: a language and environment for statistical computing. R Foundation for Statistical Computing, Vienna
- DFPRC (2014) Statistics of China's Forest Resources (2009-13). Department of Forestry of PR China, Beijing
- Dong C, Wu B, Wang C, Guo Y, Han Y (2015) Study on crown profile models for Chinese fir (*Cunninghamia lanceolata*) in Fujian Province and its visualization simulation. Scand J For Res 31:302–313. <https://doi.org/10.1080/02827581.2015.1081982>
- Dong L, Liu Z, Bettinger P (2016) Nonlinear mixed-effects branch diameter and length models for natural Dahurian larch (*Larix gmelini*) forest in northeast China. Trees 30:1191–1206. <https://doi.org/10.1007/s00468-016-1356-y>
- Farrar JRM (1987) Stem-profile functions for predicting multiple-product volumes in natural longleaf pines. South J Appl For 11:161–167. <https://doi.org/10.1093/sjaf/11.3.161>
- Feng L (2004) Method and principle in regression analysis and actual operation of SPSS. China Financial Publishing House, Beijing
- Ferreira GWD, Ferraz Filho AC, Pinto ALR, Scolforo JRS (2014) Thinning effects on taper of *Eremanthus incanus* (Less.) Less. in natural stands. Semina Ciências Agrárias 35:1707–1720. <https://doi.org/10.5433/1679-0359.2014v35n4p1707>
- Fu L, Sun H, Sharma RP, Lei Y, Zhang H, Tang S (2013) Nonlinear mixed-effects crown width models for individual trees of Chinese fir (*Cunninghamia lanceolata*) in south-central China. For Ecol Manag 302:210–220. <https://doi.org/10.1016/j.foreco.2013.03.036>

- Fu L, Sharma RP, Hao K, Tang S (2017a) A generalized interregional nonlinear mixed-effects crown width model for *Prince Rupprecht* larch in northern China. For Ecol Manag 389:364–373. <https://doi.org/10.1016/j.foreco.2016.12.034>
- Fu L, Zhang H, Sharma RP, Pang L, Wang G (2017b) A generalized nonlinear mixed-effects height to crown base model for Mongolian oak in northeast China. For Ecol Manag 384:34–43. <https://doi.org/10.1016/j.foreco.2016.09.012>
- Fu Y, He H, Zhao J, Larsen D, Zhang H, Sunde M, Duan S (2018) Climate and spring phenology effects on autumn phenology in the greater Khingan Mountains, Northeastern China. Remote Sens 10:449. <https://doi.org/10.3390/rs10030449>
- Garber SM, Maguire DA (2003) Modeling stem taper of three central Oregon species using nonlinear mixed effects models and autoregressive error structures. For Ecol Manag 179:507–522. [https://doi.org/10.1016/S0378-1127\(02\)00528-5](https://doi.org/10.1016/S0378-1127(02)00528-5)
- Gollob C, Ritter T, Vospornik S, Wassermann C, Nothdurft A (2018) A flexible height-diameter model for tree height imputation on forest inventory sample plots using repeated measures from the past. Forests 9:368. <https://doi.org/10.3390/f9060368>
- Gómez-García E, Crecente-Campo F, Diéguez-Aranda U (2013) Selection of mixed-effects parameters in a variable-exponent taper equation for birch trees in northwestern Spain. Ann For Sci 70:707–715. <https://doi.org/10.1007/s13595-013-0313-9>
- Gray HR (1956) The form and taper of forest-tree stems. University of Oxford, Oxford, UK, Imperial Forestry Institute
- Jiang L, Liu R (2011) Segmented taper equations with crown ratio and stand density for Dahurian Larch (*Larix gmelinii*) in Northeastern China. J For Res 22:347–352. <https://doi.org/10.1007/s11676-011-0178-4>
- Jiang H, Apps MJ, Peng C, Zhang Y, Liu J (2002) Modelling the influence of harvesting on Chinese boreal forest carbon dynamics. For Ecol Manag 169:65–82. [https://doi.org/10.1016/S0378-1127\(02\)00299-2](https://doi.org/10.1016/S0378-1127(02)00299-2)
- Kimmins JP, Blanco JA, Seely B, Welham C, Scoullar K (2008) Complexity in modelling forest ecosystems: how much is enough? For Ecol Manag 256:1646–1658. <https://doi.org/10.1016/j.foreco.2008.03.011>
- Kozak A (1988) A variable-exponent taper equation. Can J For Res 18:1363–1368. <https://doi.org/10.1139/x88-213>
- Kozak A (2004) My last words on taper equations. For Chron 80:507–515. <https://doi.org/10.5558/tfc80507-4>
- Kozak A, Munro DD, Smith JHG (1969) Taper functions and their application in forest inventory. For Chron 45:278–283. <https://doi.org/10.5558/tfc45278-4>
- Lappi J (1991) Calibration of height and volume equations with random parameters. For Sci 37:781–801
- Lappi J, Bailey RL (1988) A height prediction model with random stand and tree parameters: an alternative to traditional site index methods. For Sci 34:907–927. <https://doi.org/10.1093/forestscience/34.4.907>
- Larson PR (1963) Stem form development of forest trees. For Sci Monogr 5:1–42
- Leites LP, Robinson AP (2004) Improving taper equations of loblolly pine with crown dimensions in a mixed-effects modeling framework. For Sci 50:204–212. <https://doi.org/10.1093/forestscience/50.2.204>
- Lejeune G, Ung C-H, Fortin M, Guo XJ, Lambert M-C, Ruel J-C (2009) A simple stem taper model with mixed effects for boreal black spruce. Eur J For Res 128:505–513. <https://doi.org/10.1007/s10342-009-0300-8>
- Li R, Weiskittel A (2010) Comparison of model forms for estimating stem taper and volume in the primary conifer species of the North American Acadian Region. Ann For Sci 67:302. <https://doi.org/10.1051/forest/2009109>
- Li R, Weiskittel A, Dick AR, Kershaw JA, Seymour RS (2012) Regional stem taper equations for eleven conifer species in the acadian region of North America: development and assessment. North J Appl For 29:5–14. <https://doi.org/10.5849/njaf.10-037>
- Lindstrom MJ, Bates DM (1990) Nonlinear mixed effects models for repeated measures data. Biometrics 46:673–687. <https://doi.org/10.2307/2532087>
- Liu Y, Blanco JA, Wei X, Kang X, Wang W, Guo Y (2014) Determining suitable selection cutting intensities based on long-term observations on aboveground forest carbon, growth, and stand structure in Changbai Mountain, Northeast China. Scand J For Res 29:436–454. <https://doi.org/10.1080/02827581.2014.919352>
- MacPhee C, Kershaw JA, Weiskittel AR, Golding J, Lavigne MB (2018) Comparison of approaches for estimating individual tree height-diameter relationships in the Acadian forest region. Forestry 91:132–146. <https://doi.org/10.1093/forestry/cpx039>
- Max TA, Burkhart HE (1976) Segmented polynomial regression applied to taper equations. For Sci 22:283–289. <https://doi.org/10.1093/forestscience/22.3.283>
- Mehtätalo L, de-Miguel X, Gregoire TG (2015) Modeling height-diameter curves for prediction. Can J For Res 45:826–837. <https://doi.org/10.1139/cjfr-2015-0054>
- Menéndez-Miguélez M, Canga E, Álvarez-Álvarez P, Majada J (2014) Stem taper function for sweet chestnut (*Castanea sativa* Mill.) coppice stands in northwest Spain. Ann For Sci 71:761–770. <https://doi.org/10.1007/s13595-014-0372-6>
- Meng X (2006) Forest measurement, 3rd edn. China Forestry Press, Beijing
- Meng SX, Huang S (2009) Improved calibration of nonlinear mixed-effects models demonstrated on a height growth function. For Sci 55:238–248. <https://doi.org/10.1093/forestscience/55.3.238>
- Metzger K (1894) Die absoluten Schaftformzahlen der Fichte. Mundener Forstl 6:87–93
- Muhairwe CK (1993) Examination and modelling of tree form and taper over time for interior lodgepole pine. PhD thesis, University of British Columbia
- Muhairwe CK, LeMay VM, Kozak A (1994) Effects of adding tree, stand, and site variables to Kozak's variable-exponent taper equation. Can J For Res 24:252–259. <https://doi.org/10.1139/x94-037>
- Neter J, Kutner MH, Nachtsheim CJ, Wasserman W (1996) Applied linear statistical models. Irwin, Chicago
- Newberry JD, Burkhart HE (1986) Variable-form stem profile models for loblolly pine. Can J For Res 16:109–114. <https://doi.org/10.1139/x86-018>
- Newnham RM (1965) Stem form and the variation of taper with age and thinning Régime. Forestry 38:218–224. <https://doi.org/10.1093/forestry/38.2.218>
- Nigh G, Smith W (2012) Effect of climate on lodgepole pine stem taper in British Columbia, Canada. Forestry 85:579–587. <https://doi.org/10.1093/forestry/cps063>
- Njana MA, Bollandsås OM, Eid T, Zahabu E, Malimbwi RE (2016) Above- and belowground tree biomass models for three mangrove species in Tanzania: a nonlinear mixed effects modelling approach. Ann For Sci 73:353–369. <https://doi.org/10.1007/s13595-015-0524-3>
- O'Hara KL (2014) Multiaged stocking control. In: O'Hara KL (ed) Multiaged silviculture: managing for complex forest stand structures. Oxford University Press, Oxford, pp 59–83
- Omule SAY (1980) Personal bias in forest measurements. For Chron 56:222–224. <https://doi.org/10.5558/tfc56222-5>
- Ormerod DW (1973) A simple bole model. For Chron 49:136–138. <https://doi.org/10.5558/tfc49136-3>
- Özçelik R, Crecente-Campo F (2016) Stem taper equations for estimating merchantable volume of Lebanon cedar trees in the Taurus Mountains, Southern Turkey. For Sci 62:78–91. <https://doi.org/10.5849/forsci.14-212>

- Özçelik R, Brooks JR, Jiang L (2011) Modeling stem profile of Lebanon cedar, Brutian pine, and Cilicica fir in Southern Turkey using nonlinear mixed-effects models. *Eur J For Res* 130:613–621. <https://doi.org/10.1007/s10342-010-0453-5>
- Paulo JA, Tomé J, Tomé M (2011) Nonlinear fixed and random generalized height–diameter models for Portuguese cork oak stands. *Ann For Sci* 68:295–309. <https://doi.org/10.1007/s13595-011-0041-y>
- Pinheiro JC, Bates DM (2000) *Mixed-effects models in S and S-Plus*. Springer-Verlag, New York
- Pinheiro J, Bates D, DebRoy S, Sarkar D, R-Core-Team (2018) nlme: linear and nonlinear mixed effects models. R package version 3.1-137. <https://CRAN.R-project.org/package=nlme>
- Pond NC, Froese RE (2014) Evaluating published approaches for modelling diameter at breast height from stump dimensions. *Forestry* 87:683–696. <https://doi.org/10.1093/forestry/cpu029>
- Rojo A, Perales X, Sánchez-Rodríguez F, Álvarez-González JG, Kv Gadow (2005) Stem taper functions for maritime pine (*Pinus pinaster* Ait.) in Galicia (Northwestern Spain). *Eur J For Res* 124:177–186. <https://doi.org/10.1007/s10342-005-0066-6>
- Sakamoto Y, Ishiguro M, Kitagawa G (1986) Akaike information criterion statistics. D. Reidel Publishing Company, Dordrecht
- Sakici OE, Misir N, Yavuz H, Misir M (2008) Stem taper functions for *Abies nordmanniana* subsp. *bornmulleriana* in Turkey. *Scand J For Res* 23:522–533. <https://doi.org/10.1080/02827580802552453>
- Schneider R (2018) Understanding the Factors Influencing Stem Form with Modelling Tools. In: Cánovas FM, Lüttge U, Matyssek R, Pretzsch H (eds) *Progress in botany*, vol 80. Springer, Cham, pp 295–316
- Schröder T, Costa EA, Valério AF, dos Santos Lisboa G (2015) Taper Equations for *Pinus elliottii* Engelm. in Southern Paraná, Brazil. *For Sci* 61:311–319. <https://doi.org/10.5849/forsci.14-054>
- Schwarz G (1978) Estimating the dimension of a model. *Ann Stat* 6:461–464
- Scolforo HF, McTague JP, Raimundo MR, Weiskittel A, Carrero O, Scolforo JRS (2018) Comparison of taper functions applied to eucalypts of varying genetics in Brazil: application and evaluation of the penalized mixed spline approach. *Can J For Res* 48:568–580. <https://doi.org/10.1139/cjfr-2017-0366>
- SFAPRC (2011) Technical regulations for inventory for forest management planning and design [online]. <http://www.zbgb.org/Fulltext513859.htm>. Accessed 14 Jan 2011
- Sharma M, Oderwald RG (2001) Dimensionally compatible volume and taper equations. *Can J For Res* 31:797–803. <https://doi.org/10.1139/x01-005>
- Sharma M, Parton J (2009) Modeling stand density effects on taper for jack pine and black spruce plantations using dimensional analysis. *For Sci* 55:268–282. <https://doi.org/10.1093/forestsceince/55.3.268>
- Sharma M, Reid DEB (2018) Stand height/site index equations for jack pine and black spruce trees grown in natural stands. *For Sci* 64:33–40. <https://doi.org/10.5849/FS-2016-133>
- Sharma M, Zhang SY (2004) Variable-exponent taper equations for jack pine, black spruce, and balsam fir in eastern Canada. *For Ecol Manag* 198:39–53. <https://doi.org/10.1016/j.foreco.2004.03.035>
- Sharma R, Vacek Z, Vacek S (2016) Nonlinear mixed effect height–diameter model for mixed species forests in the central part of the Czech Republic. *J For Sci* 62:470–484. <https://doi.org/10.17221/41/2016-JFS>
- Smithers LA (1961) Lodgepole pine in Alberta. Bulletin 127. Canada Department of Forestry, Ottawa
- Tasissa G, Burkhart HE (1998) An application of mixed effects analysis to modeling thinning effects on stem profile of loblolly pine. *For Ecol Manag* 103:87–101. [https://doi.org/10.1016/S0378-1127\(97\)00179-5](https://doi.org/10.1016/S0378-1127(97)00179-5)
- Tasissa G, Burkhart HE, Amateis RL (1997) Volume and taper equations for thinned and unthinned loblolly pine trees in cutover, site-prepared plantations. *South J Appl For* 21:146–152. <https://doi.org/10.1093/sjaf/21.3.146>
- Trincado G, Burkhart HE (2006) A generalized approach for modeling and localizing stem profile curves. *For Sci* 52:670–682. <https://doi.org/10.1093/forestsceince/52.6.670>
- Valenti MA, Cao QV (1986) Use of crown ratio to improve loblolly pine taper equations. *Can J For Res* 16:1141–1145. <https://doi.org/10.1139/x86-201>
- Valentine HT, Gregoire TG (2001) A switching model of bole taper. *Can J For Res* 31:1400–1409. <https://doi.org/10.1139/x01-061>
- Vonesh EF, Chinchilli VM (1997) *Linear and nonlinear models for the analysis of repeated measurements*. Marcel Dekker Inc, New York
- Wang M, Kane MB, Borders BE, Zhao D (2014) Direct variance-covariance modeling as an alternative to the traditional guide curve approach for prediction of dominant heights. *For Sci* 60:652–662. <https://doi.org/10.5849/forsci.13-019>
- West PW (2009) *Tree and forest measurement*. Springer, Berlin
- Xu H (1998) *Forests in Daxing'anling Mountains China*. Science Press, Beijing
- Yang Y, Huang S (2017) Allometric modelling of crown width for white spruce by fixed- and mixed-effects models. *For Chron* 93:138–147. <https://doi.org/10.5558/tfc2017-020>
- Yang Y, Huang S, Meng SX (2009a) Development of a tree-specific stem profile model for white spruce: a nonlinear mixed model approach with a generalized covariance structure. *Forestry* 82:541–555. <https://doi.org/10.1093/forestry/cpp026>
- Yang Y, Huang S, Trincado G, Meng SX (2009b) Nonlinear mixed-effects modeling of variable-exponent taper equations for lodgepole pine in Alberta, Canada. *Eur J For Res* 128:415–429. <https://doi.org/10.1007/s10342-009-0286-2>
- Younger NL (2007) Taper, crown, and volume responses of a coastal Oregon Douglas-fir stand to sulfur treatments for control of Swiss needle cast. M.Sc. thesis, Oregon State University
- Zhao D, Wilson M, Borders BE (2005) Modeling response curves and testing treatment effects in repeated measures experiments: a multilevel nonlinear mixed-effects model approach. *Can J For Res* 35:122–132. <https://doi.org/10.1139/x04-163>

Publisher's Note Springer Nature remains neutral with regard to jurisdictional claims in published maps and institutional affiliations.

Reproduced with permission of copyright owner. Further reproduction prohibited without permission.